e-shape

EuroGEOSS Showcases: Applications Powered by Europe

S6P3 – Como City Results

The e-shape project has received funding from the European Union's Horizon 2020 research and innovation programme under grant agreement 820852

List of Authors:

Valerio Comerci [1] Pablo

Ezquerro [2]

Maria Grazia Finoia [1]

[1] Istituto Superiore per la Protezione e la Ricerca Ambientalle, ISPRA

[2] Geological Survey of Spain, IGME-CSIC

The e-shape project has received funding from the European Union's Horizon 2020 research and innovation programme under grant agreement 820852

TABLE OF CONTENTS

1 INTRODUCTION

Como city is located in the southern side of the Central Alpine Range, at the foothills of the Southern Alps, Northern Italy. The city was funded in Roman times on a flat alluvial plain located between two steep ranges (with outcropping Gonfolite Oligo-Miocene conglomerates to the W and Medolo Mesozoic limestone to the Est) and limited to the North by the shore of the Western branch of Como Lake. Only the upper ca. 150 m of the sedimentary sequence that filled the basin have been explored by boreholes. The study area is focused on the urban area (around 85,000 inhabitants), with important cultural heritage buildings and touristic assets, significant for the local economy.

The Quaternary layers that filled the basin were repeatedly modified by the erosional and depositional activity of glaciers, generating a high heterogeneity in the lithostratigraphic setting. A general synthesis of the layers can be defined as follows (Fig. 1): Unit 1, Reworked materials with archeological remains, deeper in the shore area; Unit 2, Alluvial sands and gravels; Unit 3, compressible organic silts with sandy and clayed facies, thicker towards the basin center; Unit 4, Glaciolacustrine sediments; Unit 5, Coarse deposits (Nappo et al., 2021 and references therein).

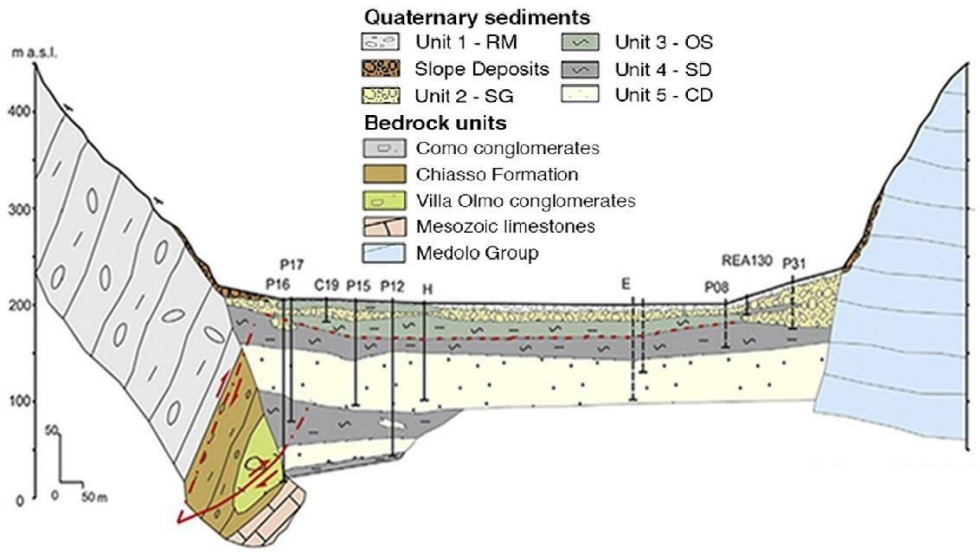

Figure 1: Geology of the basin. Figure from Nappo et al. (2021)

The hydrogeological system is composed by a shallow aquifer down to ca. 25 m deep, within anthropic and alluvial deposits and by a deeper confined aquifer in the proximal glaciolacustrine deposits, separated by a silty aquitard (Ferrario et al., 2015; Bajni et al., 2019; Binda et al., 2022). The plain is drained along its western and eastern margins by the Cosia and Valduce small creeks, which are artificially forced to flow underground before flowing into the lake. The unconfined surficial aquifer is conditioned by the fluctuation of the lake water level. The available piezometric information, related

to the surficial aquifer, collected by Insubria University from 2013 to 2015 in 33 sites and by Como Municipality in 6 piezometers near the lake shore from 22 April 2021 to 2 March 2022 shows the direct influence exerted by the lake level up to a distance from the coast of at least 100 m (Fig. 2 & 3). The strong groundwater level's dependency on the lake, which attenuates with the increasing of the distance from the lake itself, is also described by Ferrario et al. (2015) and Bajni et al. (2019).

Figure 2: Location of the piezometers surveyed by Como Municipality from April 2021 to March 2022 and Damage areas surveyed in 2022.

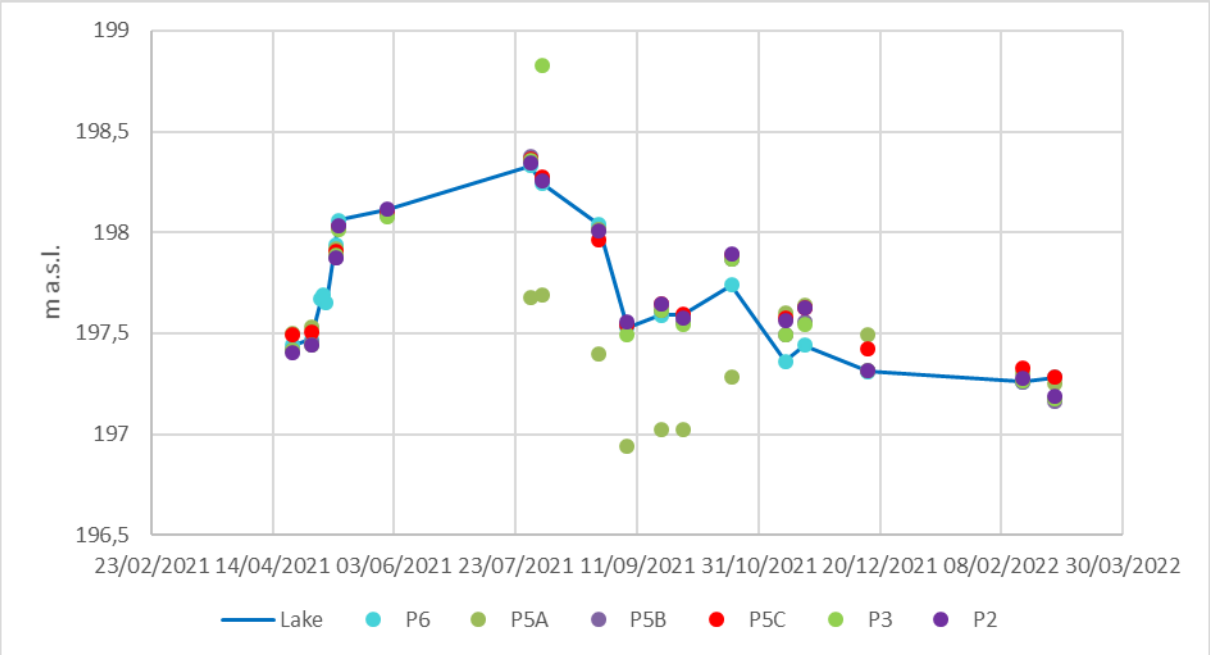

Figure 3: Water levels of the lake and piezometers of Fig. 2, from 22 April 2021 to 2 March 2022.

The urban area of Como is affected by natural and man-induced subsidence phenomena. The longterm subsidence due to the compaction of the young unconsolidated deposits shows a rate of 2-4 mm/yr (Comerci et al., 2007). After the World War II subsidence reached rates of ca. 2 cm/yr due to groundwater exploitation (Comune di Como, 1980; Comerci et al., 2007). e-Shape results aims at providing advanced analysis useful to understand the influence of the trigger and address the effects associated to the geohazard.

2 PRODUCT 1: INSAR PROCESSING

Satellite radar differential interferometry (DInSAR) is a geodetic technique that allows to remote sense small displacements of the terrestrial surface by analysing the phase differences between pairs of single look complex (SLC) SAR images. There are two methods to create the stack of interferograms. The first one uses a single reference SAR image (Single master). The second one uses a small baseline configuration, where a denser interferogram network is created linking multiple SAR images (Multimaster). The criterion to select the punctual targets in the interferograms can be simplified in amplitude and coherence methods. Amplitude selection methods work at full resolution and limit the interferometric processing only to those pixels that behave consistently over a long period of time (PS). Coherence based methods use distributed scatters (DS), or in other words, areas whose scatter

properties are not altered with time, which requires a multilook that lowers the resolution. The Small BAseline Subset (SBAS) approach (Berardino et al., 2002) is a seminal work that proposes a complete advanced DInSAR procedure using small baselines to limit the spatial decorrelation, multilooked data to reduce phase noise and a coherence-based selection criterion.

To deal with the current scenario characterized by huge SAR archives relevant to the present and future SAR missions, a parallel computing solution for the SBAS processing chain (P-SBAS) was developed (Casu et al., 2014). This step forward in optimizing computing performance was particularly suitable for web service implementation and handling big data volumes. Indeed, the P-SBAS algorithm was integrated within the Grid Processing on Demand (G-POD) environment by CNR IREA into the ESA's Geohazards Exploitation Platform (GEP). The developed on-demand web tool, which is specifically addressed to scientists that are non-expert in DInSAR data processing, permits to set up an efficient on-line P-SBAS processing service to produce surface deformation mean velocity maps and time series in an unsupervised manner (De Luca et al., 2015).

Figure 4: Mean LOS displacement velocities (PSIG). Sentinel-1, March 2015 – February 2022

The Persistent Scatterer Interferometry chain of the Geomatics (PSIG) Division of the Centre Tecnològic de Telecomunicacions de Catalunya (CTTC) described in Devanthery et al. (2014) has been used to

obtain the main results. The main steps of PSIG are: Interferogram generation; Interferogram network selection taking into account the temporal behaviour of the coherence, allowing to locate and remove interferograms with low coherence; Selection of points based on the dispersion of amplitude; Estimation of the residual topographic error and removal from original single-look interferograms; Phase unwrapping of the redundant interferograms; Atmospheric phase screening estimation using spatio-temporal filters and removal from the Time series generated in the previous step; Estimation of the velocity of deformation from the TS; Geocoding of the results. The main output of the InSAR processing stage is a deformation map composed of a set of Persistent Scatterers (PSs), with information, along the estimated Line of Sight (LOS), on the velocity of deformation and the cumulative deformation at each Sentinel-1 image acquisition time.

For the InSAR processing of the Como city the PSIG has been applied in collaboration with the CTTC. A stack of 351 images of Sentinel-1 satellite acquired from March 2015 to February 2022 in descending geometry were used (Fig. 4).

An additional InSAR dataset from the European Ground Motion Service (EGMS; https://land.copernicus.eu/pan-european/european-ground-motion-service) was analysed. Basic product was downloaded from the website including full resolution data from March 2015 to December 2021 in descending geometry (Fig. 5)

Figure 5: Mean LOS displacement velocities (EGMS). Sentinel-1, March 2015 – December 2021

Moreover, thanks to the sponsorship awarding of the project “Ground Motion in Como area” by ESA Network of Resources Initiative, it was possible to take advantage of the CNR-IREA Sentinel-1 P-SBAS Processing On-demand Service through the ESA’s Geohazards Exploitation Platform (GEP). A stack of 211 images of Sentinel-1 satellites, acquired from March 2015 to April 2022 in descending geometry, IW Mode with a spatial resolution of 90x90, have been processed (Fig. 6).

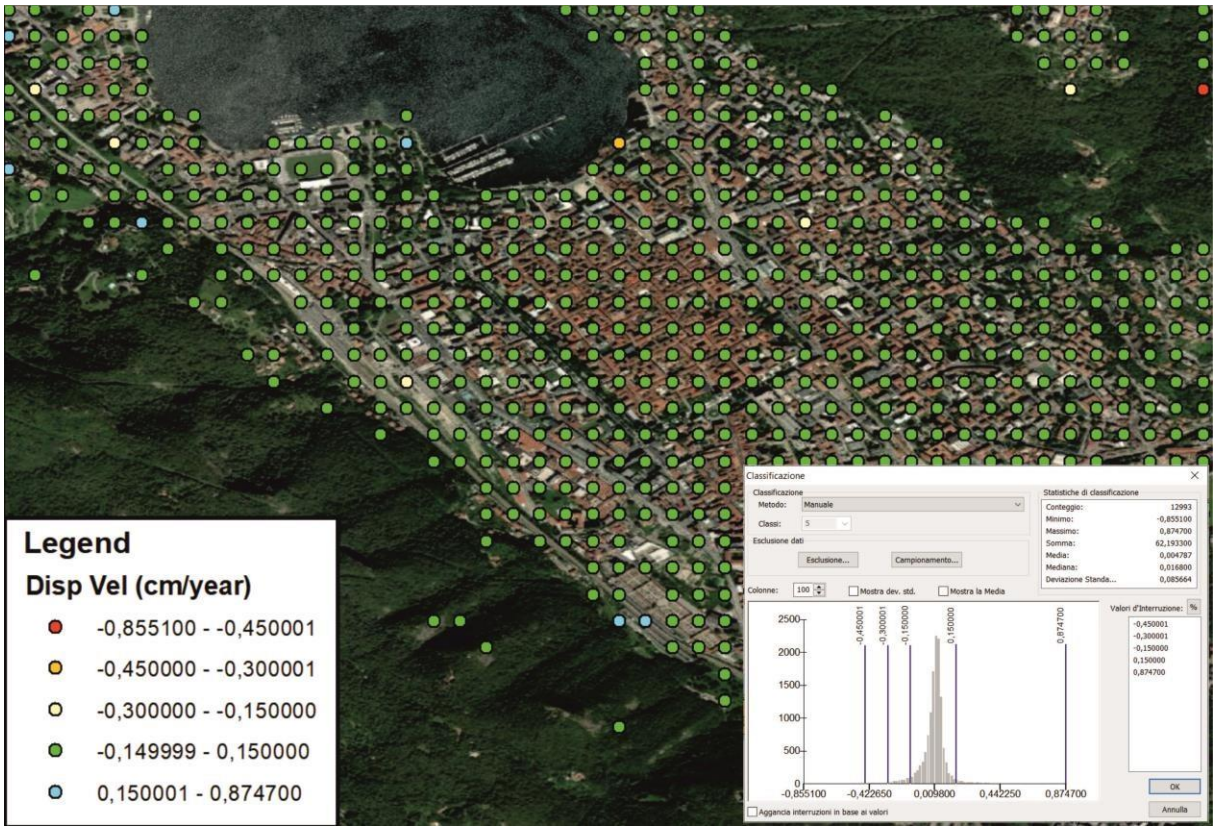

Figure 6: Mean LOS displacement velocities (GEP). Sentinel-1, March 2015 – April 2022

InSAR results show a generalized stability. Using the standard deviation of the displacement velocity, the stability threshold has been set in 1.5 mm/year. Most of the study area presents displacements below those values, making difficult a direct analysis of the results. Clusters of points with significant displacements must be evaluated locally. These areas are more numerous near the lake shore but are also detected in the center of the city. Maximum values less than 1 cm/year indicate an area with a very slow displacement trend, mostly under the capabilities of InSAR technique.

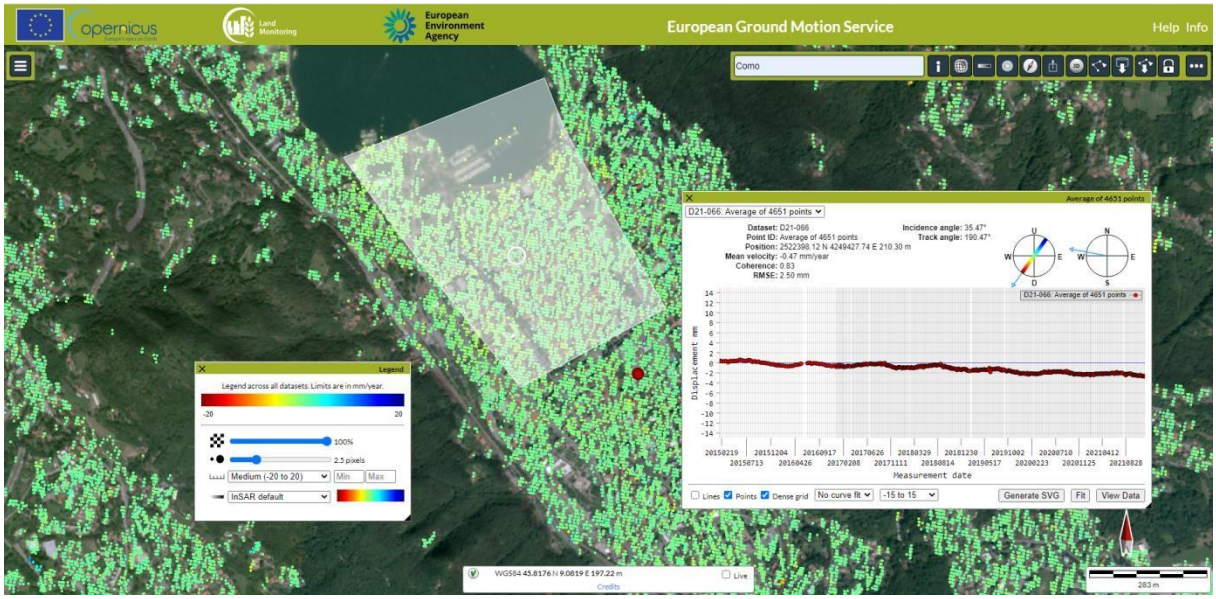

Figure 7: Mean displacement in the coastal and historical centre area assessed through the EGMS Explorer. Sentinel-1 Calibrated data (Level 2B), March 2015 – December 2021.

The analysis of the mean displacement of the coastal and historical center area (white transparent polygon in Figure 7) done through the EGMS Explorer confirms such a slow mean displacement trend.

In conclusion, the displacement map here presented, related to the March 2015 – April 2022 period, shows more stability than the displacement map elaborated by Nappo et al. (2021), based on a stack of 167 X-band Single Look Complex (SLC) SAR images acquired in Strip-map mode by CosmoSkyMed mission from June 2010 to July 2019 along descending track.

3 PRODUCT 2: INSAR VALIDATION REPORT

Validation report aims to provide validation of InSAR data based on complementary data provided by other measurement techniques. In this case study three InSAR datasets are available and quantitative validation of the results can be achieved. PSIG and EGMS datasets were used for validation.

3.1 Quantitative Validation: Partial validation using the displacement velocities

The Spatial validation requires to generate a validation grid. The new grid pixel includes around 2-4 measurement points from each original dataset, generating a 15x15 m grid. Original data were resampled to the new grid calculating the mean velocity. Those pixels without data in one of the datasets were discarded for validation (Fig. 8).

Figure 8: Absolute difference between PSIG and EGMS dataset.

Using only the active pixels for validation, some statistics can be calculated. The mean absolute difference is 0.47 mm/year, clearly below the stability threshold. The Root Mean Square Error (RMSE) is 0.73 mm/year. Calculating the relative RMSE using the Stability Threshold, this value is 49%, a medium-good accuracy value. Moreover, the R^2 shows an unsatisfactory result, 0.27. Introducing both Relative RMSE and Pearson correlation coefficient R^2 values in the accuracy matrix proposed by Navarro-Hernández et al. (2022), the conclusion would be an inaccurate result. In the analysis of this result, it must be considered that most of the displacements in Como city are under the stability threshold. Therefore, the values are noise that cannot be valorized with the R^2 statistic. If the pixel shows stability in both datasets, the accuracy is high, revealing the same result, i.e. displacements undetectable. The 94% of the compared pixels showed this behavior. Analyzing the stability of the Time series, the EGMS data present very stable time series, with variations around 3-4 mm. Meanwhile, PSIG time series variability is higher, 5 to 7 mm, but more stable in the long term. This variability, combined with the very low displacements detected, can blur validation results and analysis.

Due to this factor, the temporal validation of the results has not been calculated because it is more sensible to the noise effect.

4 PRODUCT 3: ACTIVE GEOHAZARD AREAS REPORT

Usually, InSAR processing generates thousands of points over the stability thresholds. These points may be related to a geohazard or just noisy areas due to acquisition and processing challenges associated with the technique. In this study case the problem is the opposite, only small areas are over the detection thresholds. Another aspect to keep in mind is that singular points are not significant and should not be analysed if the surrounding measurement points are not consistent or if the behaviour is not clearly validated by in-situ data.

4.1 Subsidence Report: Influence Area and Temporal evolution

It is known that the main trigger of the current subsidence phenomena in the city of Como is the presence of unconsolidated compressible sediments under the Como plain (Comerci et al., 2007; Ferrario et al., 2015; Bajni et al., 2019) and at the diverted local streams (Nappo et al., 2020).

We tried to analyse the influence of the lake levels on the ground motion with the R program, version 3.6.2 (R Core Team, 2019). The hydrometric levels of the lake measured by the hydrometer of Villa Geno from 01/03/2015 to 30/04/2022 were considered. Figure 9 shows the lake level time series decomposed into its components seasonal, trend and residuals.

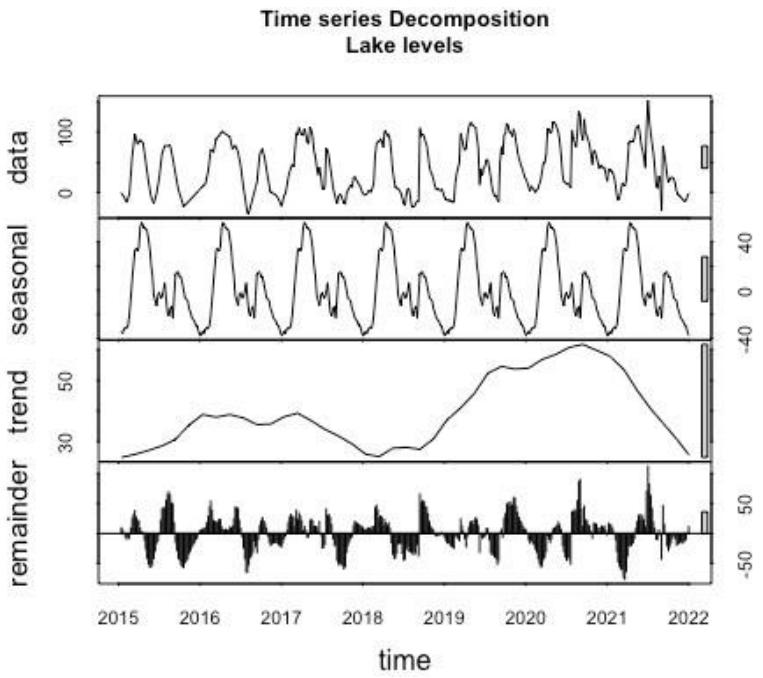

Figure 9: Lake level time series decomposed in its components seasonal, trend and residuals.

We applied the same analysis to the time series of the 40 PSs indicated in Figure 10A, all affected by subsidence in the considered period.

Figure 10: A, In light blue color the selected 40 PSs affected by subsidence in the 2015-2022 period; B, In light blue color the selected 16 PSs stable in the 2015-2022 period

Figure 11A shows the decomposition related to the PS 351, which is representative of the whole set of 40 instable PSs. Both data and trend show a constant decreasing with time. The result shows that the PSs trend seems not influenced by the lake level oscillations occurred in the analysed period. This is confirmed by the cross-correlation function represented in Figure 11B. We observe a negative correlation between the two time series for each considered time lag.

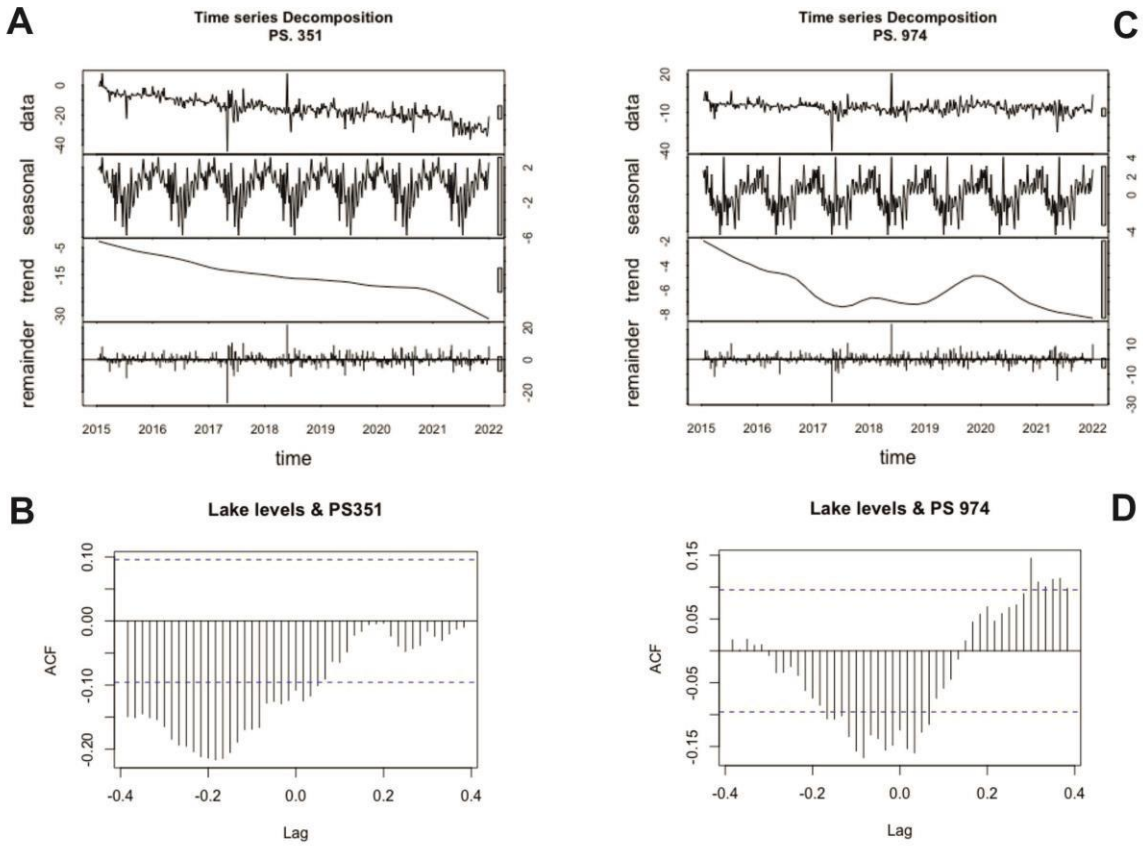

Fig. 11: A, Decomposition related to the PS 351; B, Cross-correlation between the trends of PS 351 and lake level in the whole period; C, Decomposition related to the PS 974; D, Cross-correlation between the trends of PS 974 and lake level in the whole period

We also analysed the 16 stable PSs indicated in Fig.10B. Figure 11C shows the decomposition related to the PS 974, representative of the whole set of 16 stable PSs. All the time series of such PSs show an increasing trend corresponding to the increasing of the lake level in the year 2020. The cross correlation (Fig. 11D), in fact, shows a positive correlation between the two series for positive lags. The increase or decrease of the lake level anticipates an uplifting or subsiding of the PS.

Such results seem to demonstrate that the oscillations of the lake in the considered period were not sufficient to influence the subsidence phenomena, more conditioned by geotechnical factors.

Moreover, we performed a distance analysis in order to assess the relationship between lake levels and ground motion.

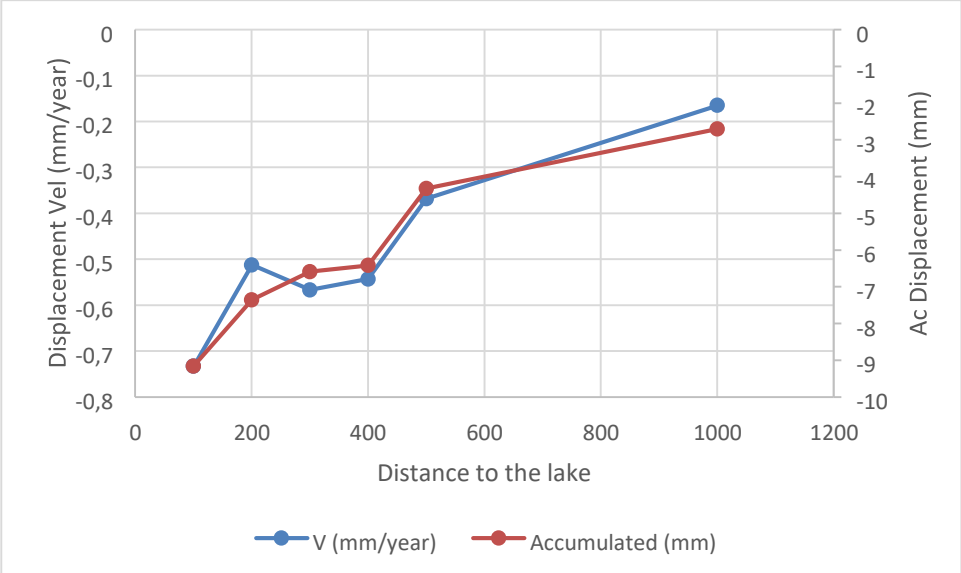

Figure 12: Displacement velocity and Cumulative displacements depending on the distance from the lake.

The shape of the lake shore was used to generate a 100-500 m buffer and calculate the mean velocity. Considering that velocities are extremely low and clearly under the stability thresholds, this analysis is also carried out using the cumulative displacements. Both results show higher displacements in the area near the lake, quickly changing at 300-400 m (Fig. 12). The inflection at 300 m from the lake is consistent with the decreasing influence of the lake level and the increasing influence of the water supply from the surrounding mountains (Ferrario et al., 2015). Even if the results are consistent, the relationship cannot be confirmed and needs to be further investigated.

In order to obtain more information to improve the analysis, the temporal evolution of the displacements at different distances has been carried out. The results of the mean accumulated displacements for each date suggest two conclusions. First, the displacements have a slight seasonal trend with 10 mm of variation, maximum values during the winter and minimum values during the summer. Second, the nearest values to the lake are slightly higher than the farther ones. Also an overall declining trend of 5 mm is suggested.

These results strength the hypothesis of certain control of the detected displacements by the lake water levels. On the other hand, the displacements are very near or below the stability thresholds making difficult to confirm the hypothesis.

5 PRODUCT 4: URBAN VULNERABLE AREAS REPORT

This product is very dependent on the available information, especially the existence of specifically designed campaigns to detect damages in the structures of the city. In this study area, one damage detection campaign was carried on, allowing the possibility to build up fragility curves.

5.1 Damage probability: Fragility curves

Previous studies over this area revealed that a significant number of buildings of the city present various levels of damages based on the approximate crack width (w) and the easy of repair, as: negligible (w < 0.1 mm); very slight (w < 1 mm); slight (w < 5 mm); and moderate (w > 5 mm) (Nappo et al., 2021). Taking into account this evidence, the clusters of points with a displacement velocity over the stability thresholds have been analysed. 17 buildings were inspected revealing different levels of damages and displacement velocities (Tab. 1). The limit of this analysis to be taken in consideration is that some buildings show only one anomalous measurement point.

Name	Damage Lvl	Displ Vel (mm/year)

3	4	-7,79
4	3-4 Building Defects	-4,65
5	2	-1,82
6	NA	-4,13
7	3	-1,48
8a	2	-1,89
8b	NA	-3,98
9a	1	-2,21
9b	3	-1,05 -
9c	4	1,5
10	4	-1,76
11	3	-2,66
12a	2	-2,55
12b	3	-1,51
12c	3	-1,52
12d	4	-1,84
A	4	-5,73

Table 1: Damage Survey data.

First, the mean displacement time series of the city center was calculated, obtaining a near stable behavior that indicates the absence of a general trend (Fig. 13). Then, the displacement time series of the surveyed buildings, including the points with displcements over 1.5 mm/year, were generated. The results showed two main patterns: one related to those buildings that present a long-term declining trend; the other related to some buildings showing a stable trend with a sharp jump. The first pattern was considered as plausible, especially if more than 4-6 measurement points show such behaviour. The second pattern may be due to a processing error, namely the phase unwrapping error. Another possible explanation for this second pattern is a sudden instability of the building but it must be supported by other information that correlates spatially and temporally with the event.

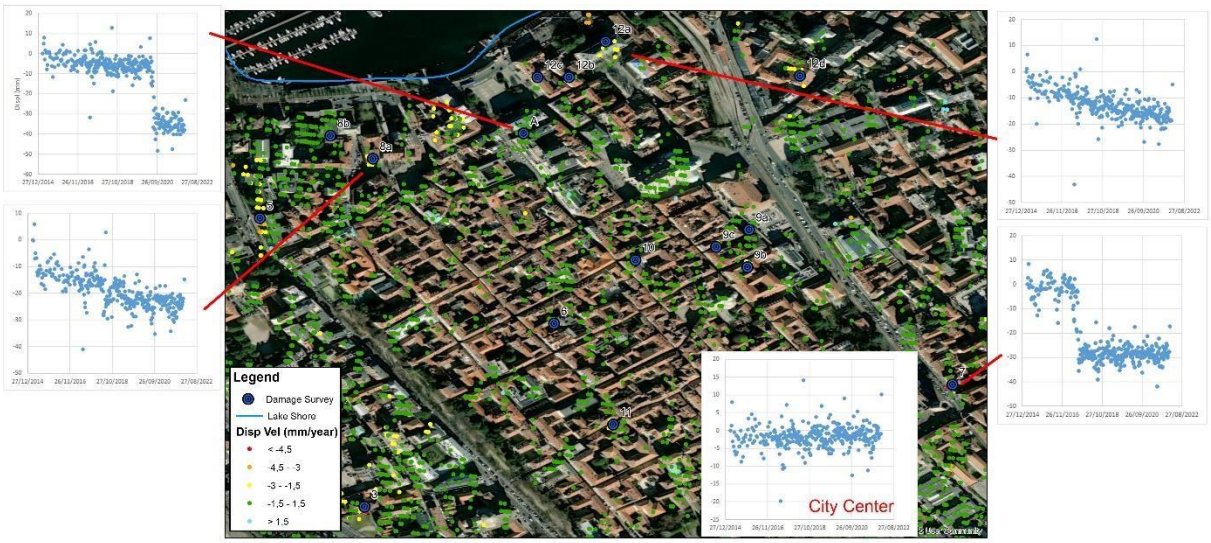

Figure 13: Cumulative displacements of the surveyed buildings.

Based on the data from the buildings with higher reliability, the fragility curves were calculated. However, considering that the displacement areas are near the stability thresholds and the distribution of the damages and clusters of detected displacements suggest that damage could be linked to the main characteristics of the buildings, the probability of damage over all the city area was not possible to be calculated because the application of the fragility curves requires the same mechanism for triggering the damage.

6 ACKNOWLEDGMENT

The Authors wish to thank M.F. Ferrario, F. Livio and A.M. Michetti (Università dell'Insubria) for their collaboration and Eng. C. Di Bartolo (Como Municipality) for providing the 2021-2022 piezometric data owned by the Municipality of Como

7 REFERENCES

Bajni G., Apuani T. & Beretta G.P., 2019. Hydro-geotechnical modelling of subsidence in the Como urban area. Eng. Geol., Vol. 257, 26 July 2019, 105144. https://doi.org/10.1016/j.enggeo.2019.105144

P. Berardino, G. Fornaro, R. Lanari, E. Sansosti, A new algorithm for surface deformation monitoring based on small baseline differential SAR interferograms, IEEE Trans. Geosci. Rem. Sens. 40 (11) (2002) 2375–2383, https://doi.org/10.1109/TGRS.2002.803792

Binda, G., Frascoli F., Spanu D., Ferrario M.F., Terrana S., Gambillara R., Trotta S., Noble P.J., Livio F., Pozzi A., Michetti A.M., 2022. Geochemical Markers as a Tool for the Characterization of a Multi-Layer Urban Aquifer: The Case Study of Como (Northern Italy). Water. 2022, 14 (1), 124. 10.3390/w14010124

Casu, F., Elefante, S., Imperatore, P., Zinno, I., Manunta, M., De Luca, C. and Lanari, R., (2014). SBASDInSAR parallel processing for deformation time-series computation. IEEE Journal of Selected Topics in Applied Earth Observations and Remote Sensing, 7(8), pp.3285-3296.

Comerci V., S. Capelletti, A.M. Michetti, S. Rossi, L. Serva, E. Vittori, Land subsidence and Late Glacial environmental evolution of the Como urban area (Northern Italy), Quat. Int. 173–174 (SUPPL) (2007) 67–86, https://doi.org/10.1016/j.quaint.2007.06.014.

Comune di Como, Relazione di sintesi della Commissione per lo Studio dei Fenomeni di Subsidenza, Documenti e Ricerche 34 (1980).

De Luca, C., Cuccu, R., Elefante, S., Zinno, I., Manunta, M., Casola, V., Rivolta, G., Lanari, R., and Casu, F., (2015). An ondemand web tool for the unsupervised retrieval of earth's surface deformation from SAR data: The P-SBAS service within the ESA G-POD environment. Remote Sensing, 7(11), pp.1563015650.

Devanthery, N., Crosetto, M., Monserrat, O., Cuevas-Gonzalez, M. & Crippa, B., 2014. An approach to Persistent Scatterer Interferometry: the PSIG chain, Remote Sens., 6, 6662–6679.

Ferrario M.F., L. Bonadeo, F. Brunamonte, F. Livio, E. Martinelli, A.M. Michetti, P. Censi Neri, V. Chiessi, V. Comerci, N. H¨obig, Late Quaternary environmental evolution of the Como urban area (Northern Italy): a multidisciplinary tool for risk management and urban planning, Eng. Geol. 193 (2015) 384–401, https://doi.org/10.1016/j.enggeo.2015.05.013.

Nappo N, M.F. Ferrario, F. Livio, A.M. Michetti, Regression analysis of subsidence in Como basin (northern Italy): new insights on natural and anthropic drivers from InSAR data, Rem. Sens. 12 (2020) 2931.

Nappo N., Peduto D., Polcari M., Livio F., Ferrario M.F., Comerci V., Stramondo S., Michetti A.M., 2021. Subsidence in Como historic centre (northern Italy): Assessment of building vulnerability combining hydrogeological and stratigraphic features, Cosmo-SkyMed InSAR and damage data. International Journal of Disaster Risk Reduction, 56, 102115. https://doi.org/10.1016/j.ijdrr.2021.102115

Navarro-Hernández M.I. et al., 2022. ValInSAR: A Systematic Approach for the Validation of Differential SAR Interferometry in Land Subsidence Areas, in IEEE Journal of Selected Topics in Applied Earth Observations and Remote Sensing, vol. 15, pp. 3650-3671, 2022, doi: 10.1109/JSTARS.2022.3171517.